

## The global impact of human activity on tropospheric ozone

H. Levy II<sup>1</sup>, P. S. Kasibhatla<sup>2</sup>, W. J. Moxim<sup>1</sup>, A. A. Klonecki<sup>3</sup>, A. I. Hirsch<sup>4</sup>,  
S. J. Oltmans<sup>5</sup>, W.L. Chameides<sup>6</sup>

**Abstract.** Within a conceptual framework of stratospheric injection, CO-CH<sub>4</sub> background tropospheric chemistry, parameterized pollution production in the continental boundary layer and surface deposition, we use an 11 level GCTM to simulate global distributions of present and pre-industrial tropospheric O<sub>3</sub>. The chemistry is driven by previously simulated present and pre-industrial NO<sub>x</sub> fields, while prescribed fields of CO, CH<sub>4</sub> and H<sub>2</sub>O are held constant. An evaluation with measurements from 12 surface sites, 21 ozonesonde sites and 1 aircraft campaign finds agreement within  $\pm 25\%$  for 73% of the observations while identifying systematic errors in the wintertime high-latitude Northern Hemisphere (NH), the Southern Hemisphere (SH) tropics during biomass burning, and the remote SH. We predict that human activity has increased the annual integral of tropospheric ozone by 39% with 3/4's of that increase in the free troposphere, though the boundary layer [BL] annual integral has increased by 66%. The 2 largest components of the global O<sub>3</sub> budget are stratospheric injection at 696 TgO<sub>3</sub>/yr, and loss through dry deposition, which increases from 459 TgO<sub>3</sub>/yr to a present level of 825 TgO<sub>3</sub>/yr. While tropospheric chemistry's net contribution is relatively small, changing from a pre-industrial destruction of -236 TgO<sub>3</sub>/yr to a present production of +128 TgO<sub>3</sub>/yr, it is a balance between two much larger terms, -558 TgO<sub>3</sub>/yr of destruction in the background troposphere and +686 TgO<sub>3</sub>/yr of production in the polluted boundary layer. Human impact on O<sub>3</sub> predominates in the summertime extratropical NH and in the tropics during their biomass burning seasons [increases of 50%-100% or more]. Conversely, there has been little increase in most of the upper troposphere [ $<20\%$ ], where ozone's influence on tropospheric climate is strongest.

### 1. Introduction

Tropospheric O<sub>3</sub>, which dominates tropospheric chemistry and may influence climate, crop production and human health, has increased by more than a factor of two in the last 100 years in the polluted boundary layer [BL] of Europe [Volz and Kley, 1988] and is frequently elevated above the natural background

in the eastern US BL [e.g., Logan, 1989]. It has been speculated that such increases have occurred throughout the NH.

Both downward transport from the stratosphere [e.g., Junge, 1962] and in situ photochemical production [e.g., Chameides and Walker, 1973; Crutzen, 1974] are believed to be important sources of tropospheric O<sub>3</sub>. Previous observation-based [e.g. Parrish et al., 1993; Moody et al., 1995] and model-based [e.g. Crutzen and Zimmermann, 1991; Jacob et al., 1993; Roelofs and Lelieveld, 1995] studies have attempted to determine the relative importance of transport and chemistry. We change the focus and present a systematic global analysis that quantifies the impact of human activity on tropospheric O<sub>3</sub> and identifies key mechanisms.

### 2. Global Chemical Transport Model (GCTM)

Our GCTM simulation is based on a conceptual model with four components controlling tropospheric O<sub>3</sub>: 1. irreversible transport of stratospheric O<sub>3</sub> into the troposphere; 2. NO<sub>x</sub>-dependent, CO-CH<sub>4</sub> based O<sub>3</sub> chemistry throughout the free troposphere and clean BL; 3. photochemical production of O<sub>3</sub> in the polluted continental BL; 4. seasonal and vegetation-dependent surface deposition of tropospheric O<sub>3</sub>.

The GCTM has a horizontal resolution of ~265 km, 11 sigma levels in the vertical at standard pressures of 10, 38, 65, 110, 190, 315, 500, 685, 835, 940, and 990 mb and is driven by twelve months of 6-hour time-averaged wind, temperature, and precipitation fields from a general circulation model. See Kasibhatla et al. [1996] and references therein for details.

Component 1, the irreversible injection of stratospheric O<sub>3</sub>, which enters the troposphere primarily at mid- and high latitudes during winter and spring [see Mahlman et al., 1980 and Levy et al., 1985 for details], and Component 4, the seasonal and vegetation-dependent surface dry deposition of O<sub>3</sub>, are treated as described in Kasibhatla et al. [1996]. Pre-industrial mid-stratospheric ozone levels remain unchanged and increased pre-industrial forestation, which may increase pre-industrial dry deposition, is neglected.

The NO<sub>x</sub>-mediated O<sub>3</sub> chemical tendencies in each gridbox in the unpolluted free troposphere and clean BL [Component 2] are interpolated each time-step from pre-calculated tables using the model's instantaneous O<sub>3</sub> levels and 6-hour average NO<sub>x</sub> levels for present and pre-industrial atmospheres taken from previous GCTM simulations. Both O<sub>3</sub> chemical tendency tables are constructed with a standard CO-CH<sub>4</sub>-NO<sub>x</sub> reaction scheme using the same climatological water vapor, temperature, CO and CH<sub>4</sub> data [Kasibhatla, 1996; Klonecki and Levy, 1997]. Detailed analyses of individual Production and Loss terms are given in Klonecki and Levy [1997]. We also include a pre-calculated O<sub>3</sub> loss from the heterogeneous nighttime conversion of NO<sub>x</sub> to HNO<sub>3</sub> on sulfate aerosol.

While pre-industrial decreases in CO, CH<sub>4</sub>, H<sub>2</sub>O, and sulfate aerosol are neglected in this study, we find that NO<sub>x</sub> dominates the O<sub>3</sub> chemical tendencies and that pre-industrial ozone tendencies are primarily destruction and not very sensi-

1. GFDL/NOAA, Princeton, New Jersey
2. Duke University, Durham, North Carolina
3. AOSP, Princeton University, Princeton, New Jersey
4. ESS, University of California, Irvine, California
5. CMDL/NOAA, Boulder, Colorado
6. EAS, Georgia Institute of Technology, Atlanta, Georgia

Copyright 1997 by the American Geophysical Union.

Paper number 97GL00599.  
0094-8534/97/97GL-00599\$05.00

tive to CO and CH<sub>4</sub> [Klonecki and Levy, 1997]. The NO<sub>x</sub> simulations, which use the same pre-calculated conversion rates among NO<sub>x</sub>, PAN and HNO<sub>3</sub>, are primarily influenced by differences between pre-industrial [ $\sim 8$  TgN/yr] and present [ $\sim 40$  TgN/yr] NO<sub>x</sub> emissions. The primary anthropogenic NO<sub>x</sub> emissions, fossil fuel combustion and biomass burning, are released in the BL of the NH midlatitudes and tropics, respectively, and produce greatly enhanced NO<sub>x</sub> levels in those regions and enhanced background levels throughout the NH. In general, the present simulated NO<sub>x</sub> levels are in good agreement with available observations [Appendix in Kasibhatla *et al.*, Table 1 and Section 3 in Levy *et al.*, 1996].

For both present and pre-industrial O<sub>3</sub>, simulated isoprene and anthropogenic NO<sub>x</sub> concentrations are used as proxies for anthropogenic and natural reactive hydrocarbons, respectively. In each grid-box, the model switches from the simple CO-CH<sub>4</sub> reaction scheme to Component 3, smog production of O<sub>3</sub>, when either NO<sub>x</sub> exceeds 200pptv or isoprene exceeds 100pptv and NO<sub>x</sub> exceeds 50 pptv. The simulation is quite insensitive to the exact magnitudes of the switches.

Because our goal is to quantify the impact of pollution O<sub>3</sub> on the global troposphere and not to simulate its local behavior in detail, we expand a simple summertime parametrization [Kasibhatla *et al.*, 1996] to reproduce seasonal-average O<sub>3</sub> levels in the polluted BL and provide a realistic source for regional and global transport. Guided by empirical relationships between NO<sub>y</sub> species and O<sub>3</sub> and theoretical calculations of O<sub>3</sub> produced per NO<sub>x</sub> consumed [e.g., Liu *et al.*, 1987; Trainer *et al.*, 1993], we relate the net rate of O<sub>3</sub> production to the rate of NO<sub>2</sub> oxidation to HNO<sub>3</sub> by OH [see Kasibhatla *et al.*, 1996]. The proportionality constant ( $k$ ) is chosen to be:

$$k(\text{NO}_x) = 8.5 \text{ for } \text{NO}_x > 1 \text{ ppbv, and} \\ k(\text{NO}_x) = [8.5 - 60 \cdot \log_{10}(\text{NO}_x)], \text{ for } \text{NO}_x < 1 \text{ ppbv.}$$

In the extratropics [30N-90N and 30S-90S], we scale  $k(\text{NO}_x)$  by  $S(\text{month})$ , which is specified using the seasonal variation of the net ozone production efficiency (OPE) calculated by Hirsch *et al.* [1996] for Harvard Forest. In the tropics [30N-30S],  $S$  is set to 1.0 throughout the year. The values of the individual parameters [8.5, 60] in  $k(\text{NO}_x)$  and  $S(\text{month})$ , while constrained by our current understanding of regional smog chemistry, are chosen to reproduce the observed seasonal levels of O<sub>3</sub> in the polluted boundary layer of the midlatitude NH and of the tropics. Significant biogenic emissions of NO<sub>x</sub> and reactive hydrocarbons induce pre-industrial BL production of O<sub>3</sub> by "pollution" Component 3, primarily in the tropics. The same  $k(\text{NO}_x)$  and  $S(\text{month})$  are used.

The parameterization is based on analyses from only a few specific geographic locations. While attempting to extrapolate to the whole globe in a rational manner, we recognize that a more global set of data and analyses is needed.

### 3. Evaluation

We compare surface, lower troposphere [surface - 800mb] and mid-troposphere [600mb - 400mb] simulations with surface, ozonesonde and aircraft measurements from around the globe. Examining the O<sub>3</sub> scatter plots in Figure 1, we see that simulation and observation agree within  $\pm 25\%$  for 144 or 73% of the cases. Another 34 or 17% fall just outside of that range. Only 20, or 10%, of the comparisons are significant outliers, and they fall into three specific categories. The first occurs during the SH biomass burning season when O<sub>3</sub> levels

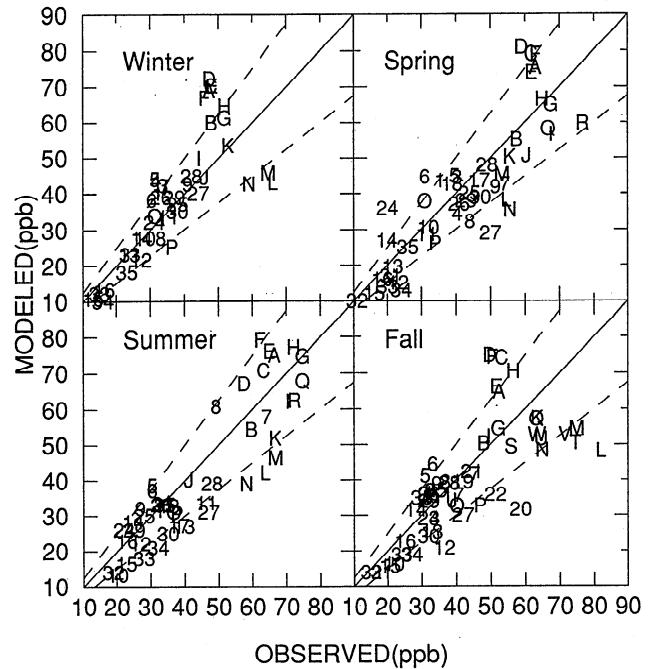


**Figure 1.** Scatter plot of simulated ozone vs. observations from 21 ozonesonde sites, 12 surface sites and the TRACE-A aircraft mission. The surface and lower troposphere [surface - 800mb] comparisons are numbers and the mid-troposphere [600 - 400mb] comparisons are letters. The sites are: Barrow, AK [1,A]; Boulder, CO [2,B]; Churchill, Can. [3,C]; Edmonton, Can. [4,D]; Goose Bay, Can. [5,E]; Resolute, Can. [6,F]; Wallops, MD [7,G]; Hohenpeissenberg, GER. [8,H]; Bermuda [9,I]; Hilo, HI [10,J]; Brazzaville, Congo [11,K]; Natal, BRZ. [12,L]; Ascension Island [13,M]; Irene, SA [14,N]; Samoa [15,O]; Lauder, NZ [16,P]; Azores [17,Q]; Canary Islands [18,R]; Cuiaba, BRZ [19,S]; Porto, BRZ [20,T]; Etosha, SA [21,U]; TRACE-A(0-30S over land) [22,V]; TRACE-A (0-30S over ocean) [23,W]; Pt. Barrow, AK [24]; Westman Island [25]; Mace Head, IR [26]; Niwot, CO [27]; Izania [28]; Bermuda [29]; Mauna Loa, HI [30]; Barbados [31]; Samoa [32]; Cape Pt., SA [33]; Cape Grim, Taz. [34]; S. Polc [35].

at Natal, Porto, and from TRACE-A aircraft over land are seriously underestimated throughout the troposphere. However, during this same period, simulated O<sub>3</sub> at Cuiaba, Etosha and over the South Atlantic compares reasonably well with measurements. The other two model biases are excess mid-troposphere O<sub>3</sub> at NH high-latitudes from September - February, which distorts the simulated seasonal cycle in that region, and the deficit at a number of island sites in the SH, particularly during the SH winter and spring. Both biases are primarily the result of stratospheric transport biases in the GCTM [Mahlman *et al.*, 1986; Levy *et al.*, 1985; and references therein].

A quantitative evaluation of the pre-industrial simulation is limited to the Paris data from the late 1800's [Volz and Kley, 1988]. While our summertime minimum is in excellent agreement, our seasonal cycle is larger.

Though far from perfect, these 3-dimensional GCTM simulations, are in harmony with the observations and capture the complex coupling between tropospheric chemistry and transport. They provide an appropriate tool for quantitative global analyses of anthropogenic impact, of transport vs. chemistry and of natural vs. pollution chemistry.

**Table 1.** Annual Integrals of Tropospheric O<sub>3</sub>

Annual Integrated O <sub>3</sub>	Present	Pre-industrial	Human Impact	
	[TgO <sub>3</sub> ]	[TgO <sub>3</sub> ]	[TgO <sub>3</sub> ]	[%]
Global Troposphere	298	215	83	39%
Free Troposphere	245	183	62	32%
NH extraTropics	93	67	26	39%
SH extraTropics	42	34	8	24%
Tropics	110	82	28	36%
Boundary Layer	53	32	21	66%
NH extraTropics	19	11	8	73%
SH extraTropics	10	7	3	43%
Tropics	24	14	10	71%

**4. Results and Discussion**

In Table 1 we predict that the total mass of tropospheric ozone has increased by 39% [83 TgO<sub>3</sub>] from a pre-industrial level of 215 TgO<sub>3</sub>. This increase, which is almost equally divided between the NH extratropics and the tropics with only a small contribution from the SH extratropics, is quite consistent with the location of human activity and related emissions. While the largest percentage increase [~70%] occurs in the BL, almost 3/4's of the actual increased mass is found in the free troposphere, requiring either export of O<sub>3</sub> from the polluted BL or enhanced background O<sub>3</sub> production.

For a more detailed picture of human impact, we examine maps of the ratios of present to pre-industrial O<sub>3</sub> for the surface and 500mb in Figures 2 and 3, respectively. The more than doubling of July surface O<sub>3</sub> over the NH mid-latitude pollution regions and of January surface O<sub>3</sub> over tropical biomass burning regions, both shown in Figure 2, should be no surprise. The doubling of July O<sub>3</sub> over most of the surface

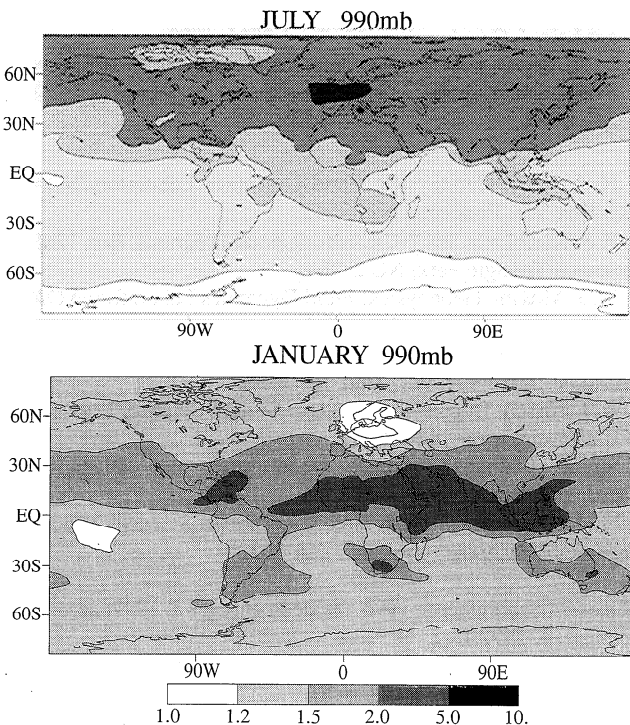


**Figure 2.** Simulated ratios of present to pre-industrial surface O<sub>3</sub> for July and January.

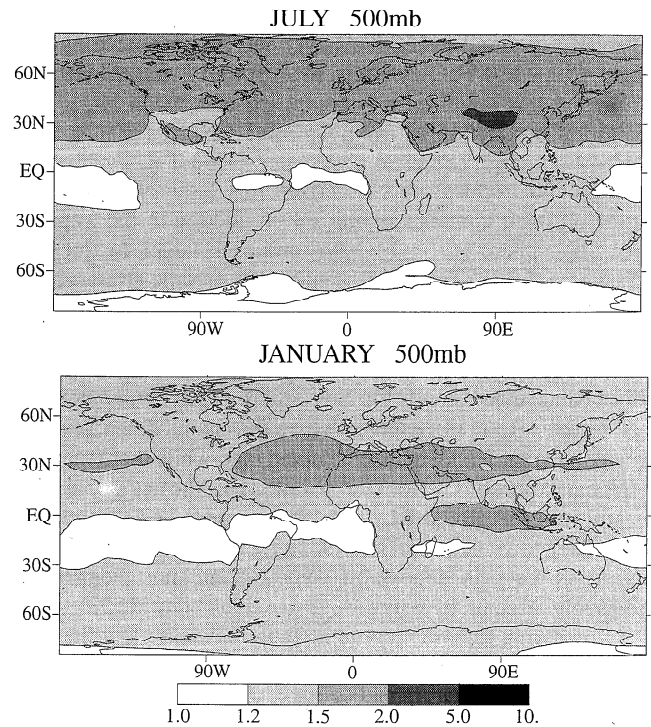


**Figure 3.** Simulated ratios of present to pre-industrial 500 mb O<sub>3</sub> for July and January.

layer of the NH, including the remote oceans, was less expected, though it is consistent with earlier speculation by *Fishman and Crutzen* [1978] and with *Volz and Kley's* [1988] extrapolation of their European data to the NH. The anthropogenic impact in the mid-troposphere shown in Figure 3 is primarily in the summer NH where O<sub>3</sub> is enhanced by more than 50%. While a NH subtropical belt of >50% enhancement remains in January, much of the wintertime NH and almost all of the SH in both July and January show only moderate levels of enhancement [20 - 50%]. Even during the SH biomass burning season [not shown] the enhancement at 500mb is <50% with the exception of a band [25S - 40S] stretching from South Africa to Australia. Human impact in the upper troposphere [not shown] is quite weak [<20%] with the exception of a 20-50% enhancement in the tropics.

In Table 2 we identify and quantify specific components or processes that control the present level of O<sub>3</sub> and that drive its increase from pre-industrial times. At present, we see that the 2 non-chemical terms, dry deposition and stratospheric injection

**Table 2.** Annual Tropospheric O<sub>3</sub> Budget

Annual O <sub>3</sub> Budget Components	Present	Pre-industrial	Human Impact
	[TgO <sub>3</sub> /yr]	[TgO <sub>3</sub> /yr]	[TgO <sub>3</sub> /yr]
Stratospheric Injection	+696	+696	0.0
CO-CH <sub>4</sub> Background Chem.	-558	-435	-123
Tropical Free Trop.	+163	+176	-13
extraTropical Free Trop.	-72	-129	+57
Boundary Layer	-649	-482	-167
B.L. Pollution Production	+686	+199	+487
Dry Deposition	-825	-459	-366

tion, still dominate, while the global integral of all chemistry is relatively small [ $+128 \text{ TgO}_3/\text{yr}$ ] and in reasonable agreement with  $+170 \text{ TgO}_3/\text{yr}$  from Roelofs and Lelieveld [1995]. However, this small term is composed of a much larger BL pollution production of  $+686 \text{ TgO}_3/\text{yr}$  which is almost balanced by a large chemical destruction [ $-558 \text{ TgO}_3/\text{yr}$ ] in the background troposphere. Moreover, this large chemical destruction itself contains significant production in the tropical free troposphere [ $+163 \text{ TgO}_3/\text{yr}$ ] and even larger destruction elsewhere [ $-721 \text{ TgO}_3/\text{yr}$ ]. Unlike the middle-stratosphere where ozone production [P] and destruction [L] tend to be in close balance [Mahlman et al., 1980; Levy et al., 1985], most of the troposphere is dominated by one term or the other. A close balance between P and L is only found in narrow boundary regions of the troposphere where the chemical tendency is changing sign. It should also be noted that, while there may be regional export of  $\text{O}_3$  from the polluted BL, the net global flux is still into the global BL, even with present levels of pollution. The global troposphere is strongly buffered from BL pollution as long as deposition velocities are not themselves adversely affected by rising  $\text{O}_3$  [e.g., Jacob et al., 1993].

Considering the 4th column in Table 2, we see that the primary human impacts, assuming no significant changes in stratospheric circulation and ozone levels, are a large increase in both BL pollution production and, as a result of increased surface  $\text{O}_3$  levels, in surface deposition. There is also a significant though smaller increase in chemical destruction in the background troposphere. Essentially, the global troposphere changes from a chemically destructive environment for  $\text{O}_3$  to a mildly productive one. This leads to significant, though regionally and seasonally variable, increases in  $\text{O}_3$  levels.

#### 4. Acknowledgments

We wish to acknowledge sounding and surface  $\text{O}_3$  data provided courtesy of E-G. Brunke and H. E. Scheel [Cape Point], I. Galbally [Cape Grim], E. Cuevas [Izania], V. W. Kirchoff [Natal], and P. Simmonds [Mace Head] and to thank J. A. Logan, J. R. Olson and the NASA/LARC EOSDIS DAAC for providing a number of  $\text{O}_3$  sounding climatologies. P. S. Kasibhatla was funded by the Atmospheric Chemistry Project of the NOAA Climate and Global Change Program under Grant NA36GP0250, and by the National Science Foundation under grant ATM-9213643.

#### References

- Chameides, W., and J. C. G. Walker, A photochemical theory of tropospheric ozone, *J. Geophys. Res.*, **78**, 8751-8760, 1973.
- Crutzen, P. J., Photochemical reaction initiated by and influencing ozone in unpolluted tropospheric air, *Tellus*, **26**, 58-70, 1974.
- Crutzen, P. J., and P. H. Zimmermann, The changing photochemistry of the troposphere, *Tellus*, **43A**, 136-151, 1991.
- Fishman, J., and P. J. Crutzen, The origin of ozone in the troposphere, *Nature*, **274**, 855-858, 1978.
- Hirsch, A. I., J. W. Munger, D. J. Jacob, L. W. Horowitz, and A. H. Goldstein, Seasonal variation of the ozone production efficiency per unit  $\text{NO}_x$  at Harvard Forest, Massachusetts, *J. Geophys. Res.*, **101**, 12659-12666, 1996.

- Jacob, D. J., et al., Factors regulating ozone over the United States and its export to the global atmosphere, *J. Geophys. Res.*, **98**, 14817-14826, 1993.
- Junge, C. E., Global ozone budget and exchange between stratosphere and troposphere, *Tellus*, **14**, 363-377, 1962.
- Kasibhatla, P. S., H. Levy II, A. A. Klonecki and W. L. Chameides, A three-dimensional view of the large-scale tropospheric ozone distribution over the North Atlantic Ocean during summer, *J. Geophys. Res.*, in press, 1996.
- Klonecki, A., and H. Levy II, Global chemical ozone tendency calculations in the troposphere, submitted to *J. Geophys. Res.*, 1997.
- Levy II, H., J. D. Mahlman, W. J. Moxim, and S. C. Liu, Tropospheric ozone: The role of transport, *J. Geophys. Res.*, **90**, 3753-3772, 1985.
- Levy II, H., W. J. Moxim, and P. S. Kasibhatla, A global 3-dimensional time-dependent lightning source of tropospheric  $\text{NO}_x$ , *J. Geophys. Res.*, **101**, 22,911-22,922, 1996.
- Liu, S. C., et al., Ozone production in the rural troposphere and the implications for regional and global ozone distributions, *J. Geophys. Res.*, **92**, 4191-4207, 1987.
- Logan, J. A., Ozone in the rural areas of the United States, *J. Geophys. Res.*, **94**, 8511-8532, 1989.
- Mahlman, J. D., H. Levy II, and W. J. Moxim, Three-Dimensional Tracer Structure and Behavior as Simulated in Two Ozone Precursor Experiments, *J. Atmos. Sci.*, **37(3)**, 655-685, 1980.
- Mahlman, J. D., H. Levy II, and W. J. Moxim, Three-Dimensional Simulations of Stratospheric  $\text{N}_2\text{O}$ : Predictions for other Trace Constituents, *J. Geophys. Res.*, **91(D2)**, 2687-2707, 1986.
- Moody, J., J. T. Merrill, S. J. Oltmans, and H. Levy II, Transport climatology for ozone in the North Atlantic, *J. Geophys. Res.*, **100**, 7179-7194, 1995.
- Parrish, D. D., J. S. Holloway, M. Trainer, P. C. Murphy, G. L. Forbes, F. C. Fehsenfeld, Export of North American ozone pollution to the North Atlantic Ocean, *Science*, **259**, 1436-1439, 1993.
- Roelofs, G.-J. and J. Lelieveld, Distribution and budget of  $\text{O}_3$  in the troposphere calculated with a chemistry general circulation model, *J. Geophys. Res.*, **100**, 20983-20998, 1995.
- Trainer, M., et al., Correlation of  $\text{O}_3$  with  $\text{NO}_y$  in photochemically aged air, *J. Geophys. Res.*, **98**, 2917-2925, 1993.
- Volz, A., and D. Kley, Evaluation of the Montsouris series of ozone measurements made in the nineteenth century, *Nature*, **332**, 240-242, 1988.

H. Levy II, Geophysical Fluid Dynamics Laboratory/NOAA  
P.O. Box 308, Princeton, NJ 08542

P. S. Kasibhatla, MCNC/Environmental Programs, Box 12889,  
Research Triangle Park, NC 27709

W. J. Moxim, Geophysical Fluid Dynamics Laboratory/NOAA  
P.O. Box 308, Princeton, NJ 08542

A. A. Klonecki, Atmospheric and Oceanic Sciences Program,  
Princeton University, Princeton, NJ 08542

A. I. Hirsch, Department of Earth System Science, University  
of California, Irvine, CA 92697

S. J. Oltmans, Climate Monitoring and Diagnostics  
Laboratory, Boulder, CO 80303

W. L. Chameides, Earth and Atmospheric Sciences, Georgia  
Institute of Technology, Atlanta, GA 30332

(Received September 6, 1996; revised February 5, 1997; accepted  
February 7, 1997.)